β cell differentiation. Mel1 $INS^{GFP/W}$ were differentiated into ß cells using the protocol previously published (1). Briefly, hESCs were dissociated to single cells with TrypLE (GIBCO). 5.5 million cells were seeded in one well of 6-well suspension plates in 5.5 mL of hESC media w/o FGF2 supplemented but with 10 ng/mL activin A (R&D Systems) and 10 ng/mL heregulinB (Peprotech) and cultured on an orbital shaker with 100 rpm speed to induce sphere formation. After 24 hours, spheres were changed with 5.5 mL Day-1 differentiation media. Media compositions: Day-1: RPMI (GIBCO) containing 0.2% FBS, 1:5,000 ITS (GIBCO), 100 ng/mL activin A, 50 ng/mL WNT3a (R&D Systems). Day-2: RPMI containing 0.2% FBS, 1:2,000 ITS, 100 ng/mL activin A. Day 3: RPMI containing 0.2% FBS, 1:1,000 ITS, 2.5 mM TGFβi IV (CalBioChem), 25 ng/mL KGF (R&D Systems). Day-4/5: RPMI containing 0.4% FBS, 1:1,000 ITS, 25 ng/mL KGF. Day-6/7: DMEM (4.5g/L glucose, GIBCO) containing 1:100 B27 (GIBCO) and 3 nM TTNPB (Sigma). Day-8: DMEM containing 1:100 B27, 3 nM TTNPB, 50 ng/mL EGF (R&D Systems). Day-9/11: DMEM containing 1:100 B27, 50 ng/mL EGF, 50 ng/mL KGF. Day-12/20: DMEM containing 1:100 B27, 1:100 Glutamax (GIBCO), 1:100 NEAA (GIBCO), 10 mM ALKi II (Axxora), 500 nM LDN-193189 (Stemgent), 1 mM Xxi (Millipore), 1 mM T3 (Sigma-Aldrich), 0.5 mM vitamin C, 1 mM N-acetyl cysteine (Sigma-Aldrich),10 mM zinc sulfate (Sigma-Aldrich), 10 mg/mL of heparin sulfate. At Day 20, clusters were dissociated into single cells using Accumax (9 min at 37°C). Live GFP^+ cells were sorted by FACS and reaggregated in Aggrewell-400 plates (StemCell Technologies) with 1.2-1.3 million cells per well of Aggrewell. The

reaggregation media (CMRL containing 10% FBS, 1:100 Glutamax, 1:100 NEAA, 10 mM ALKi II, 0.5 mM vitamin C, 1 mM T3, 1 mM N-acetyl Cysteine (Sigma-Aldrich), 10 mM zinc sulfate (Sigma-Aldrich), 10 mg/mL of heparin sulfate) supplemented with 10 mM Y-27632 (Tocris) and Penicillin/Streptomycin (Corning). Three days later, eBCs were generated and transferred to 6-well suspension plates using eBC media (reaggregration media without Y-27632 and antibiotics) and placed on an orbital shaker at 100 rpm speed. Media was changed every third day following reaggregation. eBCs were further cultured for 7-8 days prior functional assays.

Generation of INS$^{GFP/W}$ *ZNF148*-KO line. The Mel1 INS$^{GFP/W}$ *ZNF148*-KO line was generated from the INS$^{GFP/W}$ inducible Cas9 (iCas9). iCas9 was generated by integrating Neo-M2rtTA (Addgene 60843) and Puro-Cas9 (Addgene 58409) donor into the first intron of the constitutively expressed gene *PPP1R12C* at the AAVS1 locus using TALENs (AAVS1-TALEN-L (Addgene 59025) and AAVS1-TALEN-R (Addgene 59026). Briefly, Mel1 INS$^{GFP/W}$ were electroporated in the presence of 5 μg of each TALEN vector and 20 ug of the Neo-M2rtTA and Puro-Cas9 containing vector using a Biorad GenePulser (Hercules, CA), using an exponential decay, 250 V, and 500 μF. Cells were plated on plates seeded with DR4 MEFs, and two days later selected with 0.5 mg/mL Puromycin for 4 days. Survival clones were verified by PCR to select site directed integration of the targeting sequence. INS$^{GFP/W}$ iCas9 lines allow for DOX-inducible expression of Cas9 (2). sgRNA targeting exon 7 of *ZNF148* (5'-

TCTTCTCATGTCTCTGAAGC -3') was introduced by lentivirus (MOI=0.4, to allow integration of single viral copy) together with mCherry reporter. Sorted mCherry+ single cells were expanded in 2D culture to generate clones. Editing was verified by PCR followed by Sanger sequencing. Percentage of indels was calculated from the sanger sequencing traces using TIDE (Tracking of Indels by DEcomposition) (3).

Generation of inducible *S100A16* overexpression line. The Mel1 $INS^{GFP/W}$ line was edited using TALEN (see above) to introduce a DOX-inducible *S100A16* open reading frame (ORF) into the AAVS1 locus. The ORF *S100A16* (NM 080388, Origene plasmid SC120272) was first cloned into the AAVS1-TRE3G-EGFP plasmid (Addgene 52343), replacing EGFP by InFusion cloning. Electroporated cells were plated on DR4 MEFs and 2 days later selected with 0.5 mg/mL Puromycin for 4 days. Survival clones were treated with DOX and performed RT-QPCR to assess ectopic expression of *S100A16*.

siRNA knock-down in human islets. *ZNF148* knockdown in human islets was achieved by transfection of *ZNF148*-targeting siRNA (Accell Human ZNF148 7707, Horizon, A-012658-13-0005). Human islets were recovered in PRODO islet media (containing 5% human serum) for 24 hours after isolation prior transfection. Following recovery, islets were pre-incubated in Accumax for 2 min at 37°C for partial digestion to increase diffusion of Accell siRNAs throughout the islets (4). After partial digestion, PRODO media (containing 5% human serum) was added to quench digestion. Islets were then

washed in PRODO media without serum and incubated in the same medium with 1μM ZNF148-targeting siRNA or a pool of scramble siRNAs (Accell Non-Targeting Pool, Horizon, D-001910-10-05). Overnight after transfection, the media was changed to PRODO containing human serum. 3 days after siRNA transfection, the islets were collected for GSIS and RT-QPCR.

Quantitative real-time PCR. Human islets and SC-ß cells at indicated stages of differentiation were lysis in Buffer RLT Plus (Qiagen). RNA was isolated and purified using RNeasy Plus Mini (Qiagen). cDNA was synthesized using Superscript III cDNA synthesis kit (ThermoFisher). RT-qPCR was performed using 2X Sensimix SYBR Hi-ROX, on the Applied Biosystems QuantStudio 5 Real-Time PCR 384-well System. The $2^{-\Delta\Delta CT}$ method was used to calculate relative expression, after normalizing for ß-actin and/or cyclophilin-A expression.

ChIP-RTQPCR. Chromatin immunoprecipitation (ChIP) was performed using iDEAL ChIP-Seq Kit for Transcription Factors (Diagenode, C01010054) following the manufacturer's instructions with minor modifications. 20,000 IEQ were dissociated in single cells using Cell Dissociation Buffer for 30 min at 37°C. Single cells (5 million cells for each replicate ChIP) were resuspended in islet media and crosslinked with 1.1% formaldehyde for 10 min at room temperature. Glycine (1/10 volume) was added for 5 min at room temperature for quenching. Cells were pelleted, washed in 1X PBS, resuspended in ice-cold lysis buffer, and manufacturer's protocol was then followed for

the immunoprecipitation. 1.5 μg of ZNF148 antibody (ThermoFisher, A303-116A) were used for each ChIP. For each primer pair, input DNA alongside the immuno-precipitated samples and negative IgG control were run. RT-QPCR primers used are listed in Table S7.

Calcium oscillation. eBC were incubated in 3 mL of KRB containing 2.8 mM glucose and 2.5 μM Calbryte 590 AM (20701 AAT Bioquest) for 1 hour prior to loading into μ-slides for imaging (μ-slide III 3D perfusion, ibiTreat 80376). The μ-slide was located in a live imaging chamber equilibrated at 37°C under CO_2-controlled conditions. Images were taken at the UCSF Imaging core using the Zeiss Widefield, a conventional widefield microscope set upon the inverted Zeiss Axioscope 200M body. The illumination source used was a Sutter Lambda XL with appropriate excitation and emission filters for the common DAPI, FITC, TRITC. Images were taken one every 6 seconds. FITC exposure ranged between 100-120 ms. Images were taken in either static conditions (60 min in 2.8 mM glucose or 9 mM glucose), or dynamic conditions using a peristaltic pump (25 min in 2.8 mM glucose followed by 60 min in 9 mM glucose). Images were processed with custom scripts in MATLAB (MathWorks) and R. All MATLAB and R scripts are available upon request.

LC-MS/MS. eBC were incubated in MFA media (DMEM without glucose (D5030-10X1L), supplemented with 24 mM $NaHCO_3$, 10 mM HEPES, 0.2% BSA) with 8mM or

20 mM universally labelled glucose U-13C6 (Cambridge Isotope Laboratories, CLM-1396-0.25) or unlabeled glucose for 6 hours. After incubation, eBC were collected, resuspended in 150 µl ice cold quench buffer (20% methanol (Sigma 34860-2L-R), 79.9% water (Sigma 270733-1L), 0.1% formic acid (Sigma 5330020050), 3 mM NaF (Sigma S7920-100G), 1 mM phenylalanine (Sigma P5482-25G, freshly added), 100 µM EDTA), and flash frozen in liquid nitrogen. Samples were stored at -80°C until shipment to Yale IOMIC Flux Core, where LC/MS/MS was performed. Metabolite concentrations and ^{13}C-enrichments were determined by mass spectrometry using a SCIEX 5500 QTRAP equipped with a SelexION for differential mobility separation (DMS). Samples were injected onto a Hypercarb column (3µm particle size, 3x150 nM, Thermo Fisher Scientific) at a flow rate of 1 mL/min. Metabolites were eluted with a combination of aqueous (A: 15mM ammonium formate and 10uM EDTA) and organic mobile phase (B: 60% acetonitrile, 35% isopropanol and 15mM ammonium formate) according to the following gradient: t=0min, B=0%; t=0.5min, B=0%, t=1min, B=40%; t=1.5min, B=40%; t=2min, B=0%; t=6min, B=0%. Metabolite detection was based on multiple reaction monitoring (MRM) in negative mode using the following source parameters: CUR: 30, CAD: high, IS: -1500, TEM: 625, GS1: 50 and GS2: 55. DMS parameters were DT: low, MD: 2-propanol, MDC: low, DMO: 3 and DR: off, while Separation Voltage (SV) and Compensation Voltage (CoV) were optimized individually for each metabolite in order to maximize signal intensity and isobar resolution. The individual MRM transition pairs (Q_1/Q_3) are listed in Table S6. Retention times were confirmed with

known standards and peaks integrated using El-Maven. The atomic percent excess (APE) was calculated using Polly interface and corrected for background noise and for natural abundance. The sum of all measured metabolites in each sample was used as an internal control for cell density and normalization.

RNA-sequencing and data analysis. For bulk RNA-seq, total RNA was isolated using RNeasy Plus Mini kit (Qiagen). RNA quality was assessed using the Agilent Bioanalyzer Total RNA kit. Eukaryotic Strand-specific Transcriptome libraries were prepared by Novogene Corporation, and sequenced on the Illumina HiSeq instrument generating paired-end 100-base-pair reads. Read quality was assessed by FASTQC tool. Reads were mapped to Ensembl Transcriptomes v96 using Kallisto (5). Downstream analysis was performed using the program R. Differential expression analysis was performed using Sleuth. KEGG pathway analysis and Gene Ontology analysis were performed based on the set of differentially expressed genes.

For Single-cell RNA-seq, libraries were generated and sequenced at the UCSF Sequencing Core. Single cells were captured using the 10X Chromium microfluidics system (10X Genomics). Cells were encapsulated and barcoded cDNA libraries were prepared using the single-cell 3′ mRNA kit (v2 or v3; 10X Genomics). Single-cell libraries were sequenced using a NovaSeq 6000 (Illumina). The Cell Ranger software pipeline (10X Genomics, version 2.0.0, 2.1.1, or 3.0.2) was used to demultiplex cellular barcodes, map reads to the human genome (GRCh38) using the STAR aligner, and

produce a matrix of gene counts versus cells. t-distributed stochastic neighbor embedding algorithm (t-SNE) analysis was performed to identify clusters. cLoupe files generated by the Cell Ranger software pipeline were analyzed using the Loupe Cell Browser 2.0.0. Sequence Read Archive (SRA) submission: SUB12944090.

Soft X-ray tomography. eBC were incubated for 1 hour in KRB containing 2.8 mM glucose, followed by a 30 min incubation in 20 mM glucose. eBC were dissociated in single cells using Accumax (9 min at 37°C), resuspended in 20 µl of 1X PBS and loaded in thin-walled glass capillaries (1.5 µl per loading). Each capillary was rapidly plunged-frozen in nitrogen-cooled liquid propane. Projection images were collected at 517 eV using XM-2, a soft x-ray microscope at the Advanced Light Source of Lawrence Berkeley National Laboratory. The microscope was equipped with a 50-nm resolution objective lens. During data collection, cells were maintained in a stream of helium gas cooled to liquid nitrogen temperatures, which allows the collection of projection images while reducing the effects of exposure to radiation. Projection images were collected sequentially around a rotation axis of 180°, with 2° increments. Depending on the synchrotron ring current, an exposure time of 400 to 500 ms was used. The image 3D reconstruction was achieved using an iterative reconstruction method in the software package AREC3D (6).

Analysis of tomograms. For comparison, the absorption from all data was normalized and transferred to linear absorption coefficient by accounting for pixel size. All cells were manually segmented using the software Amira 2019.1. The identification of each type of organelles was based on previously published data (7) (8). The nucleus was manually segmented at first in every 10 ortho slices; each ortho slice was consequently interpolated to reconstruct the 3D label field. Mitochondria and insulin vesicles were both manually and semi-automatically segmented, setting the threshold of X-ray absorption to values previously reported (7). An average insulin vesicle LAC of 0.42 ± 0.03^{-1} μm was used to label these organelles with a range of LAC values that spans from 0.28 to 0.62 μm^{-1} was used along with morphology and size. The automatic detection of insulin granules is based on scale-space maxima of the Laplacian of the Gaussian (LoG). Granule candidates were selected as local maxima of the response in the range of 100 nm to 500 nm. From the detected local maxima, we removed all candidates with a defined semantic meaning (i.e., manually segmented instances). The detection of local maxima alone contains a large amount of false positive owing to noise in the image, as direct LoG is not susceptible to contrast. For a more representative measure, the mean granule response was defined as the sum of the LoG response of all the local maxima. The effect of noise was furtherly reduced by soft thresholding by the mean. The distance of each mean local maxima from the plasma membrane was calculated using Euclidean distance transform (EDT) and the shortest distance between the center of the maximum and the plasma

membrane was considered (9). To take into account the change in the granule response due to different cell volume, the signal was normalized by the total cell volume.

References:

1. Nair GG, Liu JS, Russ HA, Tran S, Saxton MS, Chen R, et al. Recapitulating endocrine cell clustering in culture promotes maturation of human stem-cell-derived β cells. *Nat Cell Biol.* 2019;21(2):263-74.
2. González F, Zhu Z, Shi ZD, Lelli K, Verma N, Li QV, et al. An iCRISPR platform for rapid, multiplexable, and inducible genome editing in human pluripotent stem cells. *Cell Stem Cell.* 2014;15(2):215-26.
3. Brinkman EK, Chen T, Amendola M, and van Steensel B. Easy quantitative assessment of genome editing by sequence trace decomposition. *Nucleic Acids Research.* 2014;42(22):e168-e.
4. Figueiredo H, Figueroa ALC, Garcia A, Fernandez-Ruiz R, Broca C, Wojtusciszyn A, et al. Targeting pancreatic islet PTP1B improves islet graft revascularization and transplant outcomes. *Sci Transl Med.* 2019;11(497).
5. Bray NL, Pimentel H, Melsted P, and Pachter L. Near-optimal probabilistic RNA-seq quantification. *Nature Biotechnology.* 2016;34(5):525-7.
6. Parkinson DY, Knoechel C, Yang C, Larabell CA, and Le Gros MA. Automatic alignment and reconstruction of images for soft X-ray tomography. *J Struct Biol.* 2012;177(2):259-66.
7. White KL, Singla J, Loconte V, Chen J-H, Ekman A, Sun L, et al. Visualizing subcellular rearrangements in intact β cells using soft x-ray tomography. *Science Advances.* 2020;6(50):eabc8262.
8. McDermott G, Fox DM, Epperly L, Wetzler M, Barron AE, Le Gros MA, et al. Visualizing and quantifying cell phenotype using soft X-ray tomography. *Bioessays.* 2012;34(4):320-7.
9. Loconte V, Singla J, Li A, Chen JH, Ekman A, McDermott G, et al. Soft X-ray tomography to map and quantify organelle interactions at the mesoscale. *Structure.* 2022;30(4):510-21 e3.

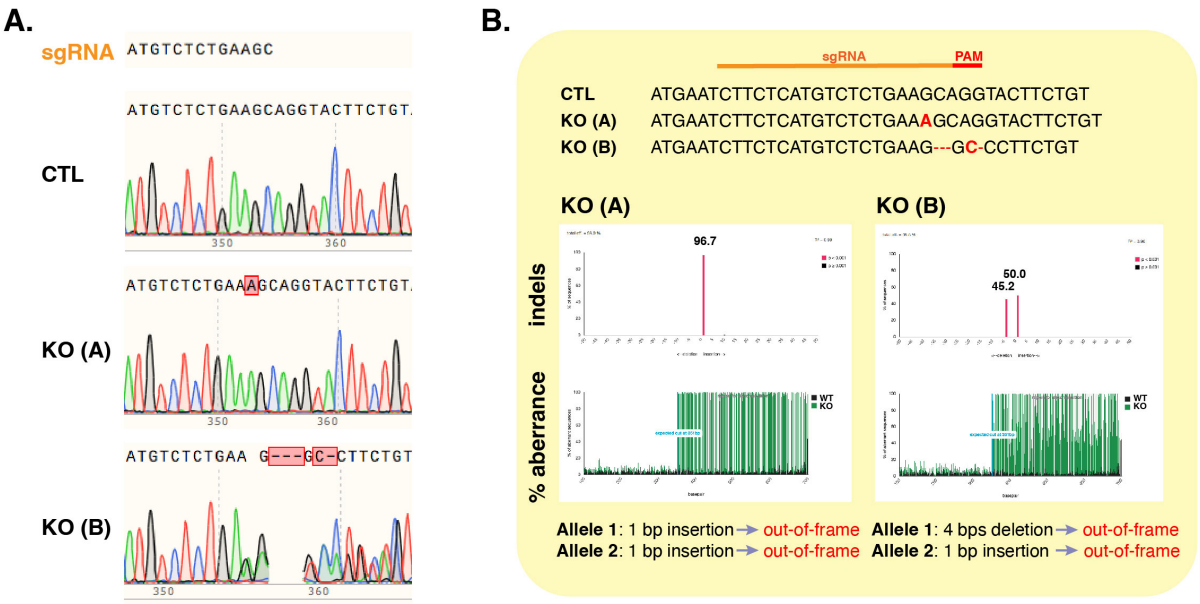

Supplemental Figure 1| Generation of *ZNF148*-KO clonal lines. (A) Sequence of sgRNA targeting *ZNF148* locus (top). Sanger sequencing data from control hESCs and CRISPR-Cas9 generated *ZNF148*-KO embryonic stem cell lines (*ZNF148*-KO clone A and B). Detected indels are indicated. **(B)** TIDE (Tracking of Indels by DEcomposition) analysis of sanger sequencing traces for *ZNF148*-KO clones (A and B). Red bar indicate position of indels and editing efficacy. A value of 0% at a position indicates that the detected nucleotide does not differ from the control sequence while a value of 100% indicates that the expected nucleotide was not detected at all. Homozygous mutations are indicated with single red bars, heterozygous mutations are indicated with two separate red bars. For each clonal line, indels are indicated for both alleles.

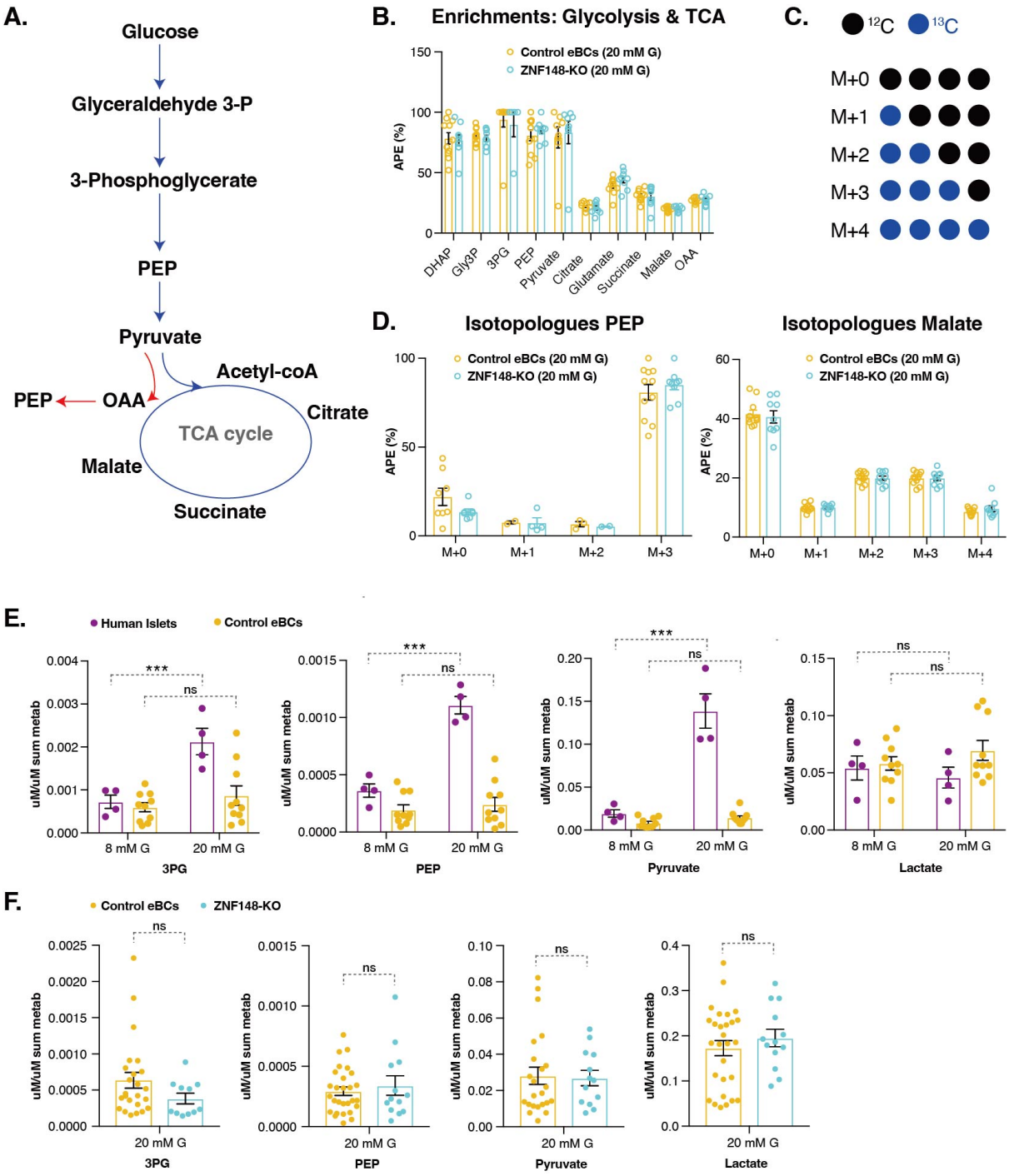

Supplemental Figure 2| Liquid chromatography tandem-mass spectrometry measurements of absolute metabolite concentrations in glycolysis and TCA cycle. (A) Schematic representation of tricarboxylic acid cycle (TCA) and glycolysis. **(B)** Atomic percent enrichment (APE) of ^{13}C through glycolysis and TCA cycle in control and *ZNF148*-KO eBC

stimulated at 20 mM glucose. n=11 independent samples for control eBC, n=9 independent samples for *ZNF148*-KO eBC. Each eBC sample contains 1.2-1.3 million cells, corresponding to ~500 eBC. **(C)** Schematic representation of ^{13}C labelling, where M+0 correspond to unlabeled substrate, and M+4 corresponds to fully labelled. **(D)** APE of PEP M+0, M+1, M+2, M+3, and malate M+0, M+1, M+2, M+3, and M+4 in control and *ZNF148*-KO eBC stimulated at 20 mM glucose. **(E)** Concentrations of glyceraldehyde 3-phosphate (3PG), phosphoenolpyruvate (PEP), pyruvate, and lactate in control eBC and cadaveric islets stimulated at 8mM or 20 mM glucose, normalized to the sum of all metabolites measured in the MIMOSA method. Data are presented as mean +/- SD. n=4 independent donors, n=10 independent samples for control eBC. Each eBC sample contains 1.2-1.3 million cells, corresponding to ~500 eBC. $^{**}P<0.001$ determined by two-tailed T-test. **(F)** Concentrations of 3PG, PEP, pyruvate and lactate in control and ZNF148-KO eBC stimulated at 20 mM glucose normalized to the sum of all metabolites measured in the MIMOSA method. Data are presented as mean +/- SD. n=10 independent samples for control eBC (n=28 technical replicates), n=4 independent samples for *ZNF148*-KO eBC (n=13 technical replicates). Each eBC sample contains 1.2-1.3 million cells, corresponding to ~500 eBC. n.s., not significant.

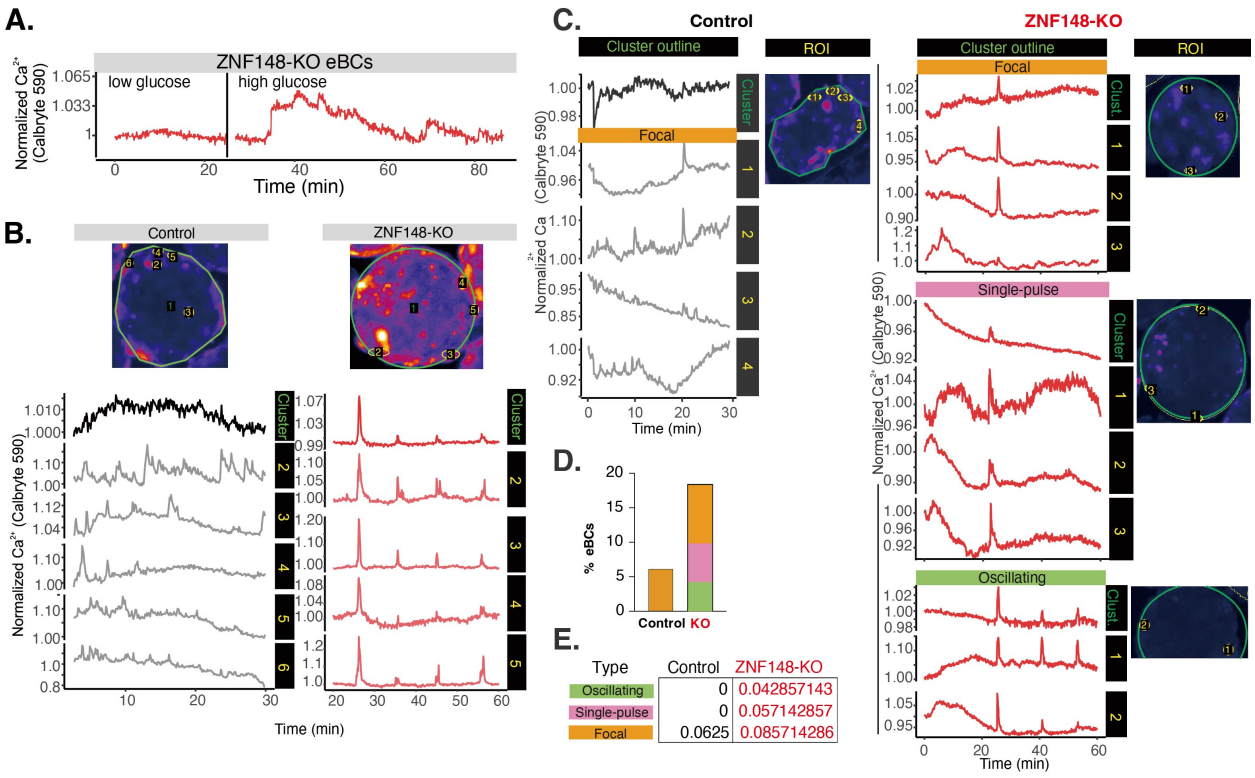

Supplemental Figure 3| Oscillatory patterns in SC-ß cells

(A) Calcium response (normalized Calbryte 590 fluorescence) in *ZNF148*-KO eBC following the transition from 2mM glucose to 9mM glucose, as indicated by the bar. **(B, C)** Signal intensity for the ROIs for the whole cluster (circled in green in image) are averaged and the individual subregions (marked by yellow numbers) are averaged, with traces shown below. **(B)** On the left panel, an example control eBC showing uncoordinated calcium responses. Each cell identified in the cluster displays unique spiking behavior regardless of its location in the cluster. On the right panel, an example of *ZNF148*-KO eBC displaying coordinated calcium activity. Traces for each subregion in the cluster is shown below the whole cluster's average trace. **(C)** Calcium response representatives of whole-cluster oscillations (type= oscillating, marked in green), whole-cluster single pulses of calcium (type= single-pulse, marked in pink), or single-pulse / oscillatory changes in only subregions of the cluster (type=focal, marked in orange) in control and *ZNF148*-

KO eBCs. *ZNF148*-KO eBCs display partial synchrony in calcium responses, including a synchronous single pulse for some regions but not observed in all of the cluster (focal), repeated calcium pulses in all regions (oscillating), or a coordinated, synchronous single spike of calcium across the whole cluster (single-pulse). Control eBCs only display a synchronous single pulse for some regions but not all of the cluster (focal). **(D, E)** Histogram **(D)** and table **(E)** showing the fraction of oscillating, single-pulse or focal type of the clusters. Fractions were determined from analyzing > 70 control and *ZNF148*-KO eBCs per experiment.

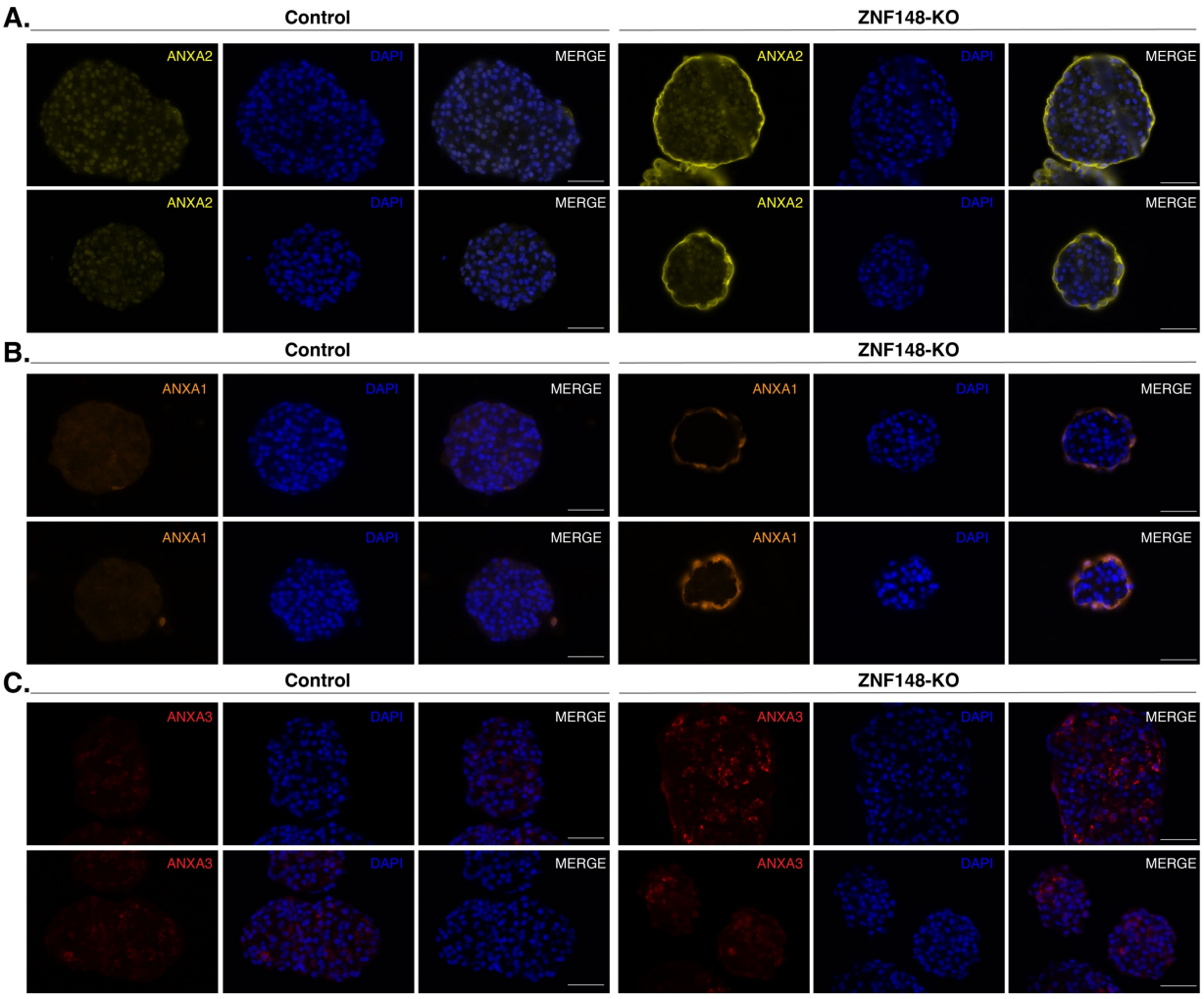

Supplemental Figure 4| Comparison of annexins localization. (A) Immunofluorescent staining of ANXA2 (yellow) in control and *ZNF148*-KO eBC. DAPI staining depicts nuclei (blue). **(B)** Immunofluorescent staining of ANXA1 (orange) in control and *ZNF148*-KO eBC. DAPI staining depicts nuclei (blue). **(C)** Immunofluorescent staining of ANXA3 (red) in control and *ZNF148*-KO eBC. DAPI staining depicts nuclei (blue). Scale bar, 50µm. Panel A and panel B show images taken from two replicates, respectively, whereas Panel C depicts overlapping images taken from the same replicate.

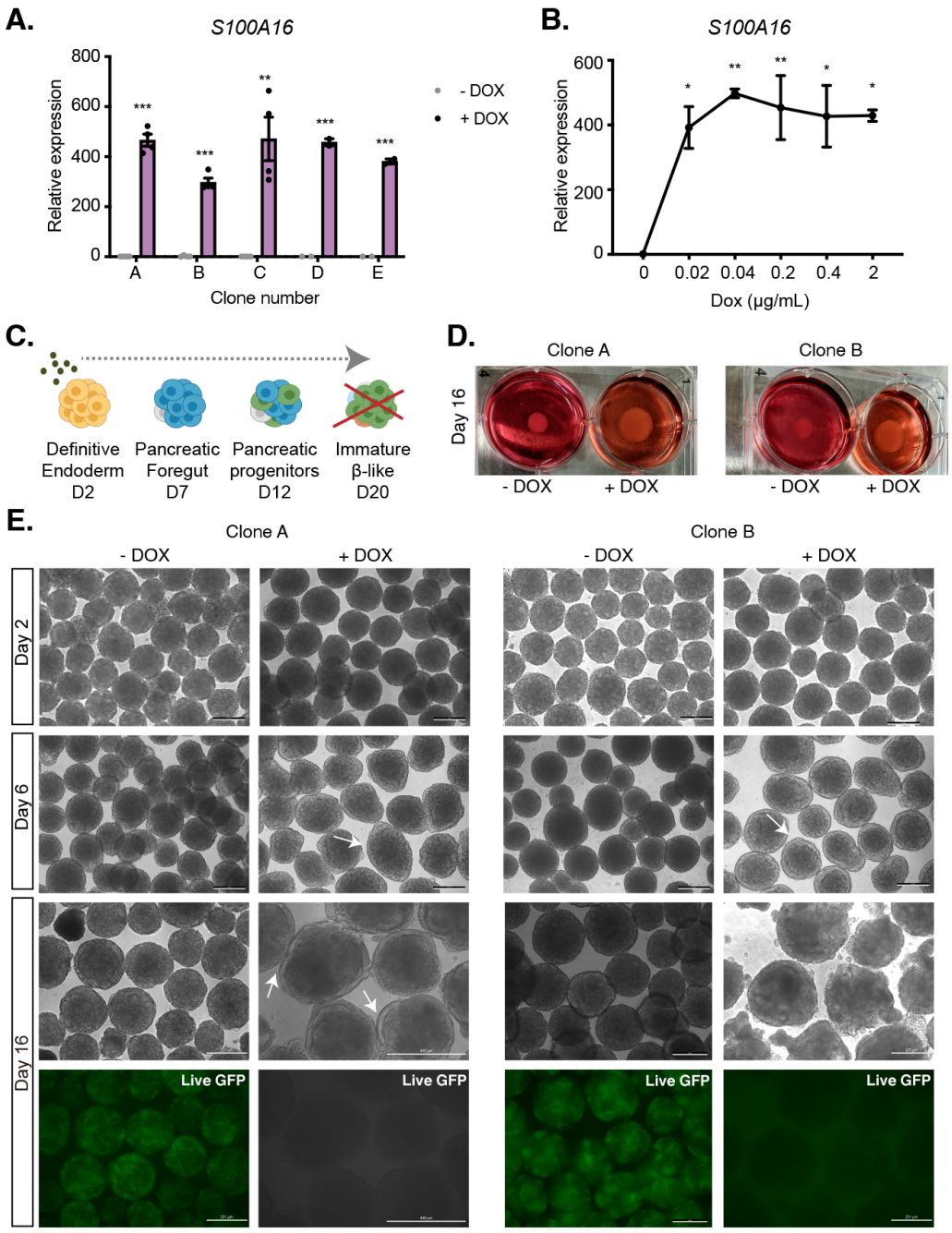

Supplemental Figure 5| Constitutive *S100A16* overexpression throughout differentiation blocks formation of insulin-positive SC-ß cells. (A) Expression levels of *S100A16* in hESC (inducible *S100A16* overexpression clonal line, INS$^{GFP/w}$ background) treated with DOX for 24 hours prior RNA extraction and QPCR measurements. Five clones (A-E) are shown. **(B)** DOX

titration analysis (clone B). n=2-4 for each group. Data are presented as mean ± s.e.m. *$P < 0.05$; **$P < 0.01$; ***$P < 0.001$; ns, not significant determined by two-tailed unpaired student's T-test. **(C)** Schematic representation of experimental design. DOX treatment starts at definitive endoderm stage (day 2) and continues over the entire differentiation. **(D)** Representative images of clusters 4 days after the pancreatic progenitor stage (day 16), with or without DOX treatment (clone A and B). **(E)** Bright-field and fluorescent representative images (clone A and B) of control clusters and S100A16-overexpressing clusters at different stages of the differentiation. Scale bar, 200μm.

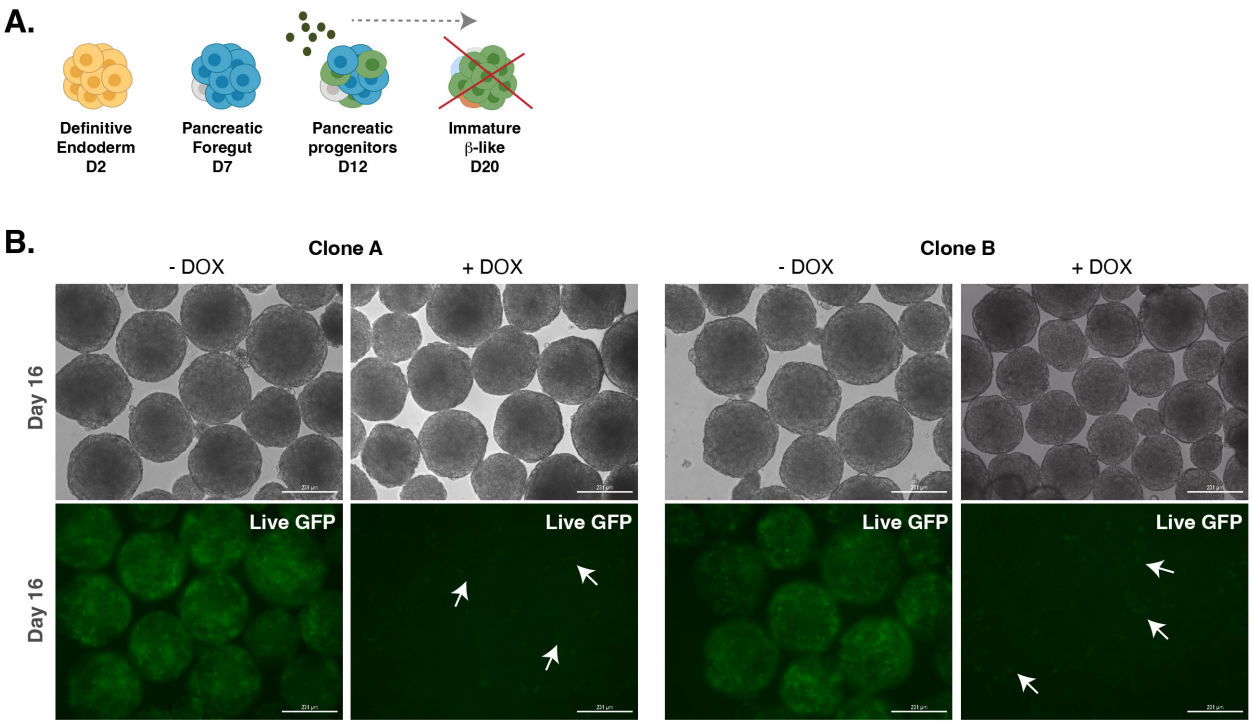

Supplemental Figure 6| *S100A16* overexpression impairs differentiation of pancreatic progenitor cells towards insulin-positive SC-ß cells. (A) Schematic representation of experimental design. DOX treatment starts at pancreatic progenitor stage (day 12) and continues over the entire differentiation. **(B)** Bright-field and fluorescent representative images (clone A and B) of control clusters and *S100A16*-overexpressing clusters 4 days after DOX treatment. Scale bar, 200µm.

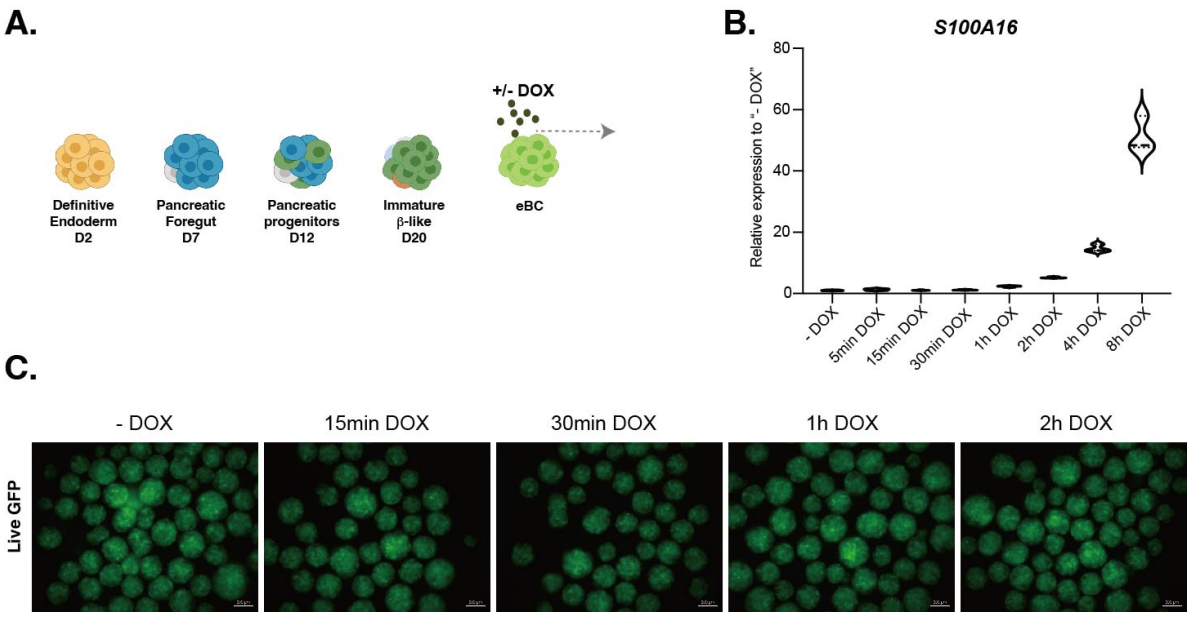

Supplemental Figure 7| Optimization of DOX treatment in eBCs to keep *S100A16* overexpression in a physiological range. (A) Schematic representation of experimental design. DOX treatment starts at eBC stage (Day 26). At each time point (5 min, 15 min, 30 min, 1 h, 2 hrs, 4 hrs and 8 hrs), DOX treated eBCs are washed with PBS and continue culturing until the "8h DOX" group finishes the DOX treatment. Then eBCs of all DOX conditions are collected for qPCR analysis. **(B)** Expression levels of S100A16 in Clone A eBCa after DOX treatment shown in **(A).** n=3 **(C)** INS-GFP fluorescent representative images show Clone A eBCs 2 days after DOX treatment. Scale bar, 200μm.